



Evaluating carbon fluxes of global forest ecosystems by using an individual tree-based model FORCCHN



Jianyong Ma^{a,b}, Herman H. Shugart^c, Xiaodong Yan^{b,*}, Cougui Cao^a, Shuang Wu^b, Jing Fang^b

^a MOA Key Laboratory of Crop Eco-physiology and Farming System in the Middle Reaches of the Yangtze River/College of Plant Science and Technology, Huazhong Agricultural University, Wuhan 430070, China

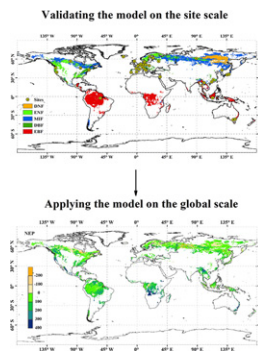
^b State Key Laboratory of Earth Surface Processes and Resource Ecology, Beijing Normal University, Beijing 100875, China

^c Department of Environmental Sciences, University of Virginia, Charlottesville, VA 22904, USA

HIGHLIGHTS

- FORCCHN can account for a substantial amount of the variability in observed CO₂ flux across worldwide EC sites.
- FORCCHN could be used to evaluate carbon fluxes of forest ecosystems on global scale.
- FORCCHN simulations predict that global forest ecosystems are a carbon storage with NEP value being $2.20 \pm 0.64 \text{ Pg C yr}^{-1}$.

GRAPHICAL ABSTRACT



ARTICLE INFO

Article history:

Received 23 September 2016

Received in revised form 8 February 2017

Accepted 8 February 2017

Available online 15 February 2017

Editor: Elena Paoletti

Keywords:

Individual tree-based model FORCCHN

Eddy-covariance

Gross primary production

Ecosystem respiration

Net ecosystem production

Forest ecosystems

ABSTRACT

The carbon budget of forest ecosystems, an important component of the terrestrial carbon cycle, needs to be accurately quantified and predicted by ecological models. As a preamble to apply the model to estimate global carbon uptake by forest ecosystems, we used the CO₂ flux measurements from 37 forest eddy-covariance sites to examine the individual tree-based FORCCHN model's performance globally. In these initial tests, the FORCCHN model simulated gross primary production (GPP), ecosystem respiration (ER) and net ecosystem production (NEP) with correlations of 0.72, 0.70 and 0.53, respectively, across all forest biomes. The model underestimated GPP and slightly overestimated ER across most of the eddy-covariance sites. An underestimation of NEP arose primarily from the lower GPP estimates. Model performance was better in capturing both the temporal changes and magnitude of carbon fluxes in deciduous broadleaf forest than in evergreen broadleaf forest, and it performed less well for sites in Mediterranean climate. We then applied the model to estimate the carbon fluxes of forest ecosystems on global scale over 1982–2011. This application of FORCCHN gave a total GPP of 59.41 ± 5.67 and an ER of $57.21 \pm 5.32 \text{ Pg C yr}^{-1}$ for global forest ecosystems during 1982–2011. The forest ecosystems over this same period contributed a large carbon storage, with total NEP being $2.20 \pm 0.64 \text{ Pg C yr}^{-1}$. These values are comparable to and reinforce estimates reported in other studies. This analysis highlights individual tree-based model FORCCHN could be used to evaluate carbon fluxes of forest ecosystems on global scale.

© 2017 Elsevier B.V. All rights reserved.

* Corresponding author at: Jingshi Keji Building B-811, NO.12 Xueyuan South Road, Haidian District, Beijing Normal University, Beijing 100875, China.
E-mail address: yxd@bnu.edu.cn (X. Yan).

1. Introduction

Forest ecosystems are important components of the terrestrial carbon cycle because of their ability to store much larger amounts of carbon (C) than other terrestrial ecosystems (McKinley et al., 2011; Gray and Whittier, 2014). Land ecosystems represent an important C sink that annually removes from the atmosphere approximately 29% of the global fossil-fuel and land-use-change emissions (Le Quéré et al., 2009). Accurate quantification of the C budget, its dynamics and its drivers in forest ecosystems is a critical component of efforts to reduce greenhouse gas emissions and mitigate the effects of projected climate change through forest C management (White et al., 2005; Seidl et al., 2012; Russell et al., 2015). Although forest-inventory databases offer the potential for estimating the regional ecosystem C budgets in some locations, ecological models have proven to be essential tools for expanding the coverage of these data. This is usually accomplished through model simulations based on maps of the driving environmental variables and site conditions. For remote-sensing data sets, ecological models have found application in interpreting C fluxes from observations into estimates for C cycle studies. These models vary in their level of abstraction and also in the spatial resolution used in their applications.

The most models, including TEM (McGuire et al., 1992), BIOME-BGC (Running and Hunt, 1993), CENTURY (Parton et al., 1993), CASA (Potter et al., 1993), IBIS (Foley, 1994), SiB2 (Sellers et al., 1996), LPJ (Sitch et al., 2003) and ORCHIDEE (Krinner et al., 2005), have been developed to assess or project forest ecosystems processes by considering fundamental processes (photosynthesis, respiration, etc.) and aggregated state variables (e.g. living plant tissue, soil organic carbon storage, etc.) shared across all terrestrial ecosystems as a paradigm for simulation. In general, the dynamic equations are parameterized to represent relatively large areas (~0.1° to ~0.5° latitude × longitude blocks). The characteristics and critical driving factors of the C budget vary across different terrestrial ecosystems. These differences may be exacerbated depending on differences in the structure and internal functions across ecosystems. This has led to applications of other model formulations with increased complexity. Hence, several individual-based and stand-based models for forest ecosystems have been developed to investigate the C cycle scaling up from on patch-scale consideration, for instance, Hybrid (Friend et al.,

1997), LoTEC (King et al., 1997), LPJ-GUESS (Smith et al., 2001), TRIPLEX (Peng et al., 2002), and INTCARB (Song and Woodcock, 2003). Because they include detailed descriptions of population dynamic processes, such as establishment, mortality and the effects of resource competition on individual growth, these models not only describe tree biomass dynamics with greater elaboration (Friend et al., 1997; Smith et al., 2001; Zhao et al., 2012), but they also have more details in the resolution of structural features of forests such as canopy heights, average diameters of trees and the statistical distributions of these variables. Such predictions potentially allow the models to be tested or calibrated against data produced through recent advances in remote-sensing technology (Shugart et al., 2015).

In general, to achieve a correct soil C storage and reasonable forest initial condition, most process-based C models are “spun-up” for 500–1000 years when the soil C storage becomes stable, and the landscape structure develops from a bare-soil starting condition to an assumed quasi-equilibrium vegetation. Note, however, that the quasi-equilibrium landscape derived from simulation represents an idealized status, rather than real forest condition. Based on this reason, Yan and Zhao (2007) proposed utilizing measurement-based inventory data to characterize the forest initial condition for C cycle simulations, and implemented this in developing the individual tree-based FORest-ecosystem-Carbon-budget-model-for-CHiNa (FORCCHN). Due to the difficulties in collecting inventory data on regional scale, they used satellite-derived LAI products to initialize the necessary vegetation, including the estimate of how many trees gets planted on plot scale and what growth state of individual tree could achieve (e.g. tree height), and then FORCCHN was successfully applied to simulate the C cycle over China (Yan and Zhao, 2007; Zhao et al., 2012).

The current paper tests how well the FORCCHN model captures the spatial-temporal variations of gross primary production (GPP), ecosystem respiration (ER) and net ecosystem production (NEP) over the FLUXNET dataset. Our goals are to: (1) examine model performance across a global network of flux sites for the first time, and (2) apply FORCCHN to estimate the C fluxes of forest ecosystems on global scale for the past 30 years. Such quantification of the C uptake capacity in forest ecosystems provides a scientific foundation for predicting future changes in atmosphere CO₂ and climate, and for defining management options for the global C cycle (Yu et al., 2014).

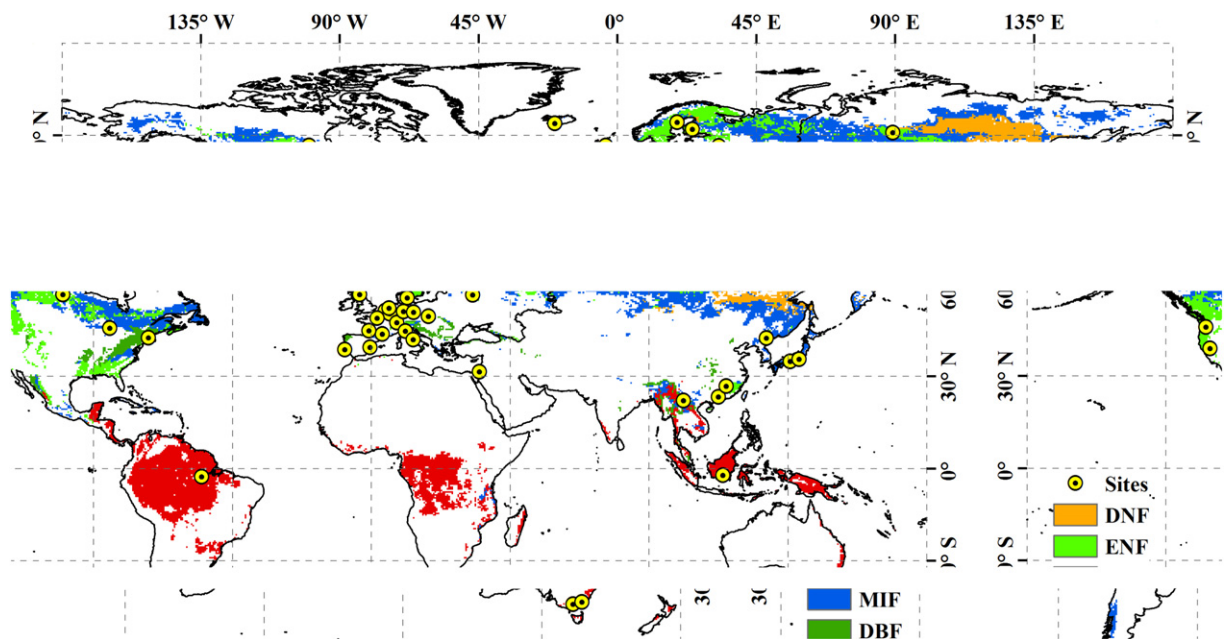


Fig. 1. Spatial distribution of studied EC sites and global forest types based on International Geosphere Biosphere Program-Data and Information Service (IGBP-DIS) DISCover land cover classification system. DNF, ENF, MIF, DBF and EBF denote deciduous needleleaf forest, evergreen needleleaf forest, mixed forest, deciduous broadleaf forest and evergreen broadleaf forest, respectively.

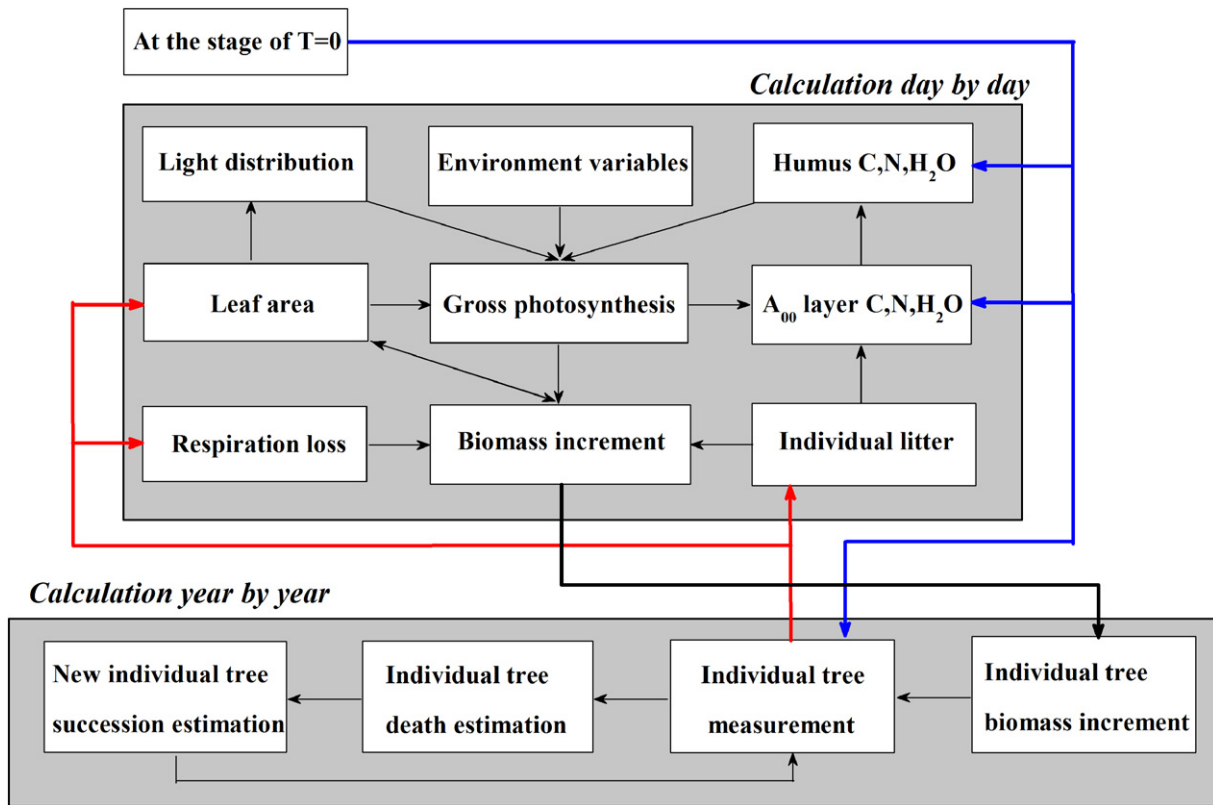


Fig. 2. The primary processes and flow charts of the FORCCHN model.

2. Materials and methods

2.1. Eddy covariance data

The Eddy covariance (EC) technique allows measuring directly net ecosystem CO₂ exchange (NEE) relative to an area (the footprint) of hundreds of meters around EC tower. NEE and NEP have the same absolute values but opposite signs. Data gaps due to sensors malfunctioning or less than ideal turbulence conditions (Papale et al., 2006) are filled using different gap-filling methods (artificial neural network and marginal distribution sampling techniques) described in Papale and Valentini (2003) and Reichstein et al. (2005). The two main components of C fluxes (GPP and ER) are estimated using the flux-partitioning technique based on the extrapolation of night-time flux observations with temperature dependent relations (Reichstein et al., 2005). The daily EC data used in this study are obtained from the LaThuile FluxNet free use dataset (<http://www.fluxdata.org>), AmeriFlux (<http://ameriflux.ornl.gov>), European Fluxes Database (<http://www.europe-fluxdata.eu>), ChinaFlux (<http://www.chinaflux.org>) and FFPRI FluxNet (<http://www2.ffpri.affrc.go.jp/labs/flux/index.html>). We simply selected the main sites with typical geographical distribution and longer measured time series, and a total of 37 EC sites located between ~38°S to ~70°N in latitude are chosen to evaluate the FORCCHN model. The sites cover four major forest types: evergreen broadleaf forest (EBF), deciduous broadleaf forest (DBF), mixed forest (MIF), and evergreen needleleaf forest (ENF). Details about the EC sites, the years of available data and their characteristics as well-corresponding forest types and Köppen climate classification are provided in Fig. 1 and Table S1 (Supplement).

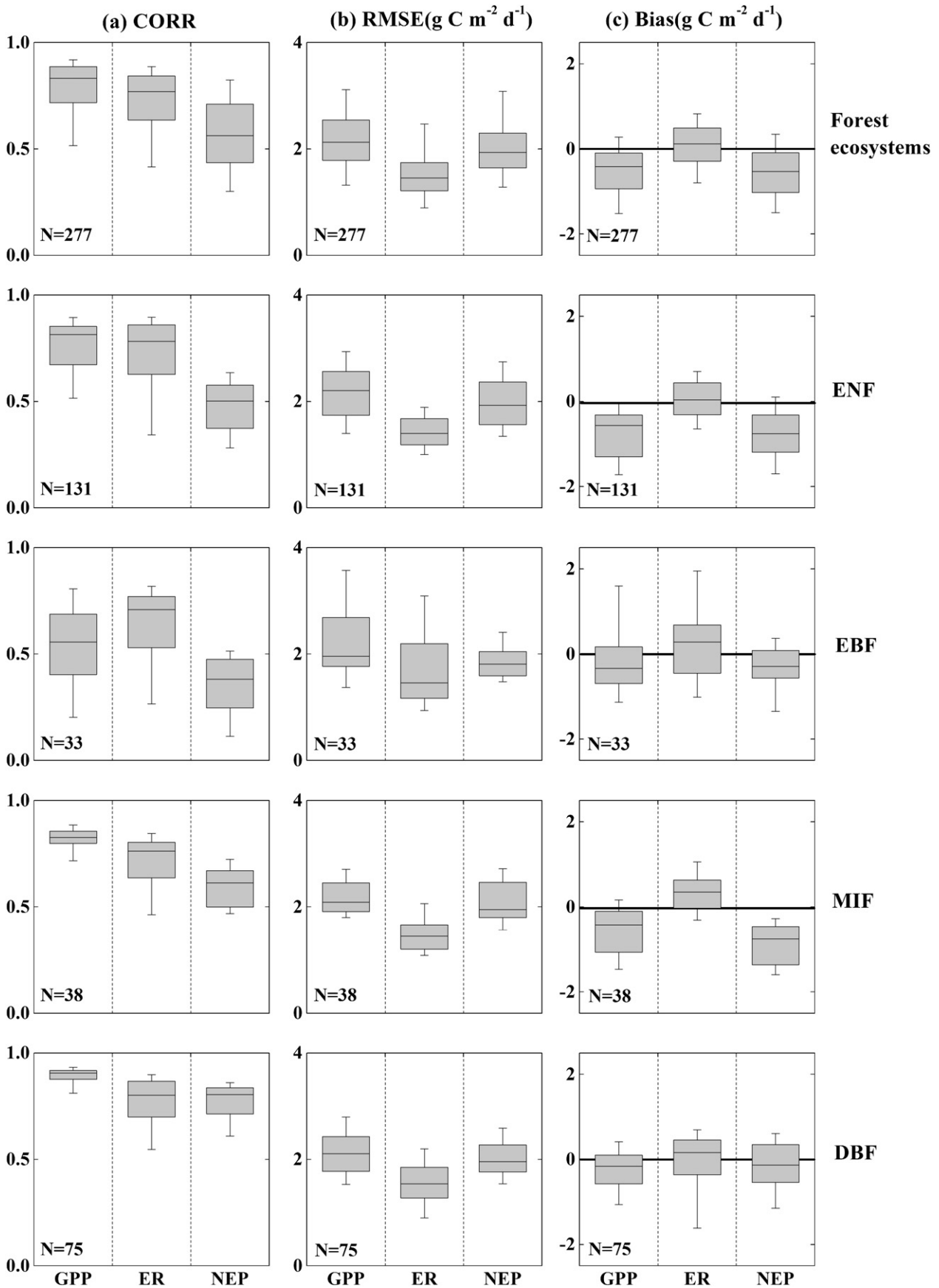
2.2. FORCCHN model description

The individual tree-based model, FORCCHN, is driven by daily meteorological data and simulates forest seasonal and interannual carbon

budget by coupling soil C cycle models on plot scale (~600 m²). Depending on the process considered, FORCCHN runs on daily and annual time steps (Fig. 2). For an individual tree, the principal daily processes are photosynthesis, maintenance respiration, photosynthate allocation, nitrogen (N) uptake, as well as soil organic matter (SOM) decomposition and N mineralization. Model assumes that net photosynthate is only allocated to the growth and the litter of leaves and fine roots, while the rest of photosynthate is stored in a so-called ‘buffer carbon pool’ in daily process. At the end of the year, the cumulative ‘buffer carbon pool’ is mainly used to support the growth of canopy height and diameter at breast height (DBH), and the production of coarse wood debris (CWD). Note that if the death occurs in a given year, the C, N from litter fall and mortality would completely transfer to the soil pools at the end of the year, and continue to participate in new C, N cycle in the coming year (Yan and Zhao, 2007). The modelling soil C and N dynamics in FORCCHN are established based on modified CENTURE sub-model (Kirschbaum and Paul, 2002). In brief, it includes above- and below-ground litter pools, woody litter pools and three SOM pools (active, slow and resistant) with different respective decomposition rates.

Table 1
Parameters of soil decomposition rate in the FORCCHN model.

Symbol	Unit	Carbon pool	Value
S ₁	d ⁻¹	Above-ground metabolic litter pool	0.080
S ₂	d ⁻¹	Above-ground structural litter pool	0.021
S ₃	d ⁻¹	Below-ground metabolic litter pool	0.100
S ₄	d ⁻¹	Below-ground structural litter pool	0.027
S ₅	d ⁻¹	Fine woody litter pool	0.010
S ₆	d ⁻¹	Coarse woody litter pool	0.002
S ₇	d ⁻¹	Below-ground coarse litter pool	0.002
S ₈	d ⁻¹	Active soil organic matter pool	0.040
S ₉	d ⁻¹	Slow soil organic matter pool	0.001
S ₁₀	d ⁻¹	Resistant soil organic matter pool	3.5 × 10 ⁻⁵



Fluxes of N are parallel those of C. The litter pool decomposition parameters described in Kirschbaum and Paul (2002) are listed in Table 1.

Taking the shade tolerant (ST) and intolerant (SIT) species into consideration along with tree and other generic characteristics, an individual tree is assumed in FORCCHN to belong to one of the nine plant functional types (PFTs): rain forest trees (ST and SIT), evergreen broadleaf trees (ST and SIT), deciduous broadleaf trees (ST and SIT), evergreen needleleaf trees (ST and SIT) and deciduous needleleaf trees. The corresponding physiological and ecological parameters of each PFTs are listed in Table S2 (Supplement). It is important to realize that these parameters are essentially qualitative and mostly quantitative descriptors of the attributes of an idealized tree of each functional type. For these reasons, while the parameters can certainly be changed, they are not free parameters to be fitted arbitrarily.

2.3. Model driving data

2.3.1. Climate input

The climate forcing used in this study includes the daily maximum and minimum air temperature (°C), precipitation (mm), relative humidity (%), wind speed (m/s), atmospheric pressure (hPa) and total solar radiation (W/m²). For model validation, daily meteorological data with the observed C flux are all obtained from the corresponding EC sites (Section 2.1). For global simulation, climate inputs are derived through a combination of reanalysis data and observations, and are available from Princeton University over the 1982–2011 period at a grid resolution of 0.5° × 0.5° (<http://hydrology.princeton.edu>) (Sheffield et al., 2006).

2.3.2. Soil parameters

Soil parameters are composed of the soil organic matter (carbon and nitrogen pool in units of kg C/m² and kg N/m², respectively) and soil physical parameters. The soil physical parameters, which are strongly dependent on the geographical position, include the soil field capacity (mm), wilting point (mm), bulk density (kg/m³), sand content (%), silt content (%) and clay content (%). In the study, the Global Gridded Surfaces of Selected Soil Characteristics (Global Soil Data Task Group, 2000) coupled with Harmonized World Soil Database (Nachtergaele et al., 2012) provides resources for the soil organic matter and physical parameters.

2.3.3. Satellite-derived vegetation products

Global forest types are derived from International Geosphere Biosphere Program-Data and Information Service (IGBP-DIS) DISCover land cover classification system, with a spatial resolution of 0.5° × 0.5° (Loveland et al., 2009) (Fig. 1). The 8-day 5-km LAI of Global Land Surface Satellite (GLASS) in 1982 (Liang et al., 2013) is also used to drive the model. Quality control flags in LAI are applied to screen and reject poor quality data by product developers. The 8-day LAI are composited into the yearly maximum and minimum values. Note that satellite-derived LAI datasets are resampled to the geographic projection and spatial resolution of the global climate input.

2.3.4. CO₂ data

The monthly mean values of the atmospheric carbon dioxide concentration derived from Mauna Loa Observatory, Hawaii, USA during 1982–2011 are used to drive the model, and the data are downloaded from the website of Carbon Dioxide Information Analysis Center(<http://cdiac.ornl.gov/>).

2.4. Model validation

The model performance is quantified in several ways. For the site scale simulations, the simulated GPP, ER and calculated NEP from simulated GPP and ER are compared against observed data using correlation coefficient (CORR), the root mean square error (RMSE), efficiency (E) (Weglarczyk, 1998; Balzarolo et al., 2014) and bias:

$$CORR = \frac{\sum_{i=1}^n (S_i - \bar{S})(O_i - \bar{O})}{\sqrt{\sum_{i=1}^n (S_i - \bar{S})^2 \sum_{i=1}^n (O_i - \bar{O})^2}} \quad (1)$$

$$RMSE = \sqrt{\frac{1}{n} \sum_{i=1}^n (S_i - O_i)^2} \quad (2)$$

$$E = \frac{\sum_{i=1}^n (O_i - \bar{O})^2 - \sum_{i=1}^n (S_i - O_i)^2}{\sum_{i=1}^n (O_i - \bar{O})^2} \times 100\% \quad (3)$$

$$Bias = \frac{1}{n} \sum_{i=1}^n (S_i - O_i) \quad (4)$$

where S_i and O_i are daily simulated and observed fluxes, respectively, \bar{S} and \bar{O} represent their averages. The E value can range from $-\infty$ to 100%, and a value close to 100% indicates a perfect match between the simulated and observed data. A negative value occurs when the observed average is a better predictor than the simulation.

To analyze the annual variability of C fluxes, the absolute anomalies are calculated using annual cumulative data:

$$Anomaly_{yr} = \left| \frac{Flux_{yr} - \overline{Flux}}{\overline{Flux}} \right| \times 100\% \quad (5)$$

where $Flux_{yr}$ denotes cumulative flux for year (yr) and \overline{Flux} is the average annual cumulative flux for all available years.

3. Results

3.1. Simulation performance by IGBP forest types

In general, the FORCCHN model could reproduce the observed C fluxes of forest ecosystems across all 37 EC site (Fig. 3, Table 2). The greatest CORR value with a small interquartile range is observed in GPP (CORR = 0.72) across all forest types, followed by ER (CORR = 0.70) and NEP (CORR = 0.53), indicating that NEP is more difficult to represent among the three C fluxes in our simulations. There is an underestimation in our model for GPP and NEP, with averaged bias values of $-0.41 \text{ g C m}^{-2} \text{ d}^{-1}$ and $-0.46 \text{ g C m}^{-2} \text{ d}^{-1}$, respectively (Fig. 3c, Table 2).

For GPP and ER, the greatest CORR value occurs in deciduous broadleaf forest and mixed forest. Evergreen broadleaf forest not only has the lowest CORR value, but it also shows the largest interquartile range in RMSE (Fig. 3b). This means that our model has relatively less predictive ability for GPP and ER for evergreen broadleaf forest. In terms of bias, FORCCHN often underestimates the GPP but slightly overestimates the ER across most forest types.

For NEP, the simulation represents well in deciduous broadleaf forest and mixed forest because of the higher CORR values, but the poorest

Fig. 3. Performance of the FORCCHN in simulating daily GPP (gross primary production), ER (ecosystem respiration) and NEP (net ecosystem production) across forest types on a site × year basis: (a) CORR- correlation coefficient, (b) RMSE- root mean square error, (c) Bias. Panel figure from top to bottom is Forest ecosystems, ENF (evergreen needleleaf forest), EBF (evergreen broadleaf forest), MIF (mixed forest) and DBF (deciduous broadleaf forest), respectively. Forest ecosystems represent all four categories. The tops and bottoms of each 'box' are the 25th and 75th percentiles of the samples, respectively. The line in the middle of each box denotes the median value. The upper and lower whiskers are the 5th and 95th percentiles of the samples, respectively. N is number of available years.

Table 2
Performance of the FORCCHN in simulating daily carbon fluxes for all forest types.^a

Forest types	N. site	N. data	GPP					N. sites E > 50%	ER					N. sites E > 50%	NEP					
			CORR	RMSE	-O	-S	Bias		CORR	RMSE	-O	-S	Bias		CORR	RMSE	-O	-S	Bias	
ENF	16	44,658	0.70	2.01	3.67	2.98	-0.69	7	0.69	1.38	2.76	2.82	0.06	7	0.46	1.95	0.91	0.16	-0.75	0
EBF	8	11,714	0.51	1.98	6.01	5.93	-0.08	1	0.65	1.89	5.73	5.85	0.12	0	0.41	1.78	0.28	0.08	-0.20	0
MIF	5	13,119	0.80	2.27	4.00	3.55	-0.45	4	0.68	1.61	2.78	3.12	0.34	2	0.56	2.20	1.22	0.43	-0.79	1
DBF	8	25,666	0.88	1.99	3.87	3.66	-0.21	8	0.78	1.44	2.97	2.93	-0.04	4	0.75	1.91	0.90	0.73	-0.17	5
Forest ecosystems	37	95,157	0.72	2.01	4.26	3.85	-0.41	20	0.70	1.53	3.45	3.50	0.05	13	0.53	1.94	0.81	0.35	-0.46	6

^a N. site-number of available sites for each forest type; N. data-number of available days; CORR-correlation coefficient; RMSE-root mean square error ($\text{g C m}^{-2} \text{d}^{-1}$); -O- average of observation ($\text{g C m}^{-2} \text{d}^{-1}$); -S-average of simulation ($\text{g C m}^{-2} \text{d}^{-1}$); Bias ($\text{g C m}^{-2} \text{d}^{-1}$); N. sites E > 50%-number of sites with model efficiency (E) higher than 50%; Forest ecosystems represent all four categories.

performance is found in evergreen broadleaf forest with CORR being much lower than 0.5. The simulated errors in both GPP and ER could impact the uncertainty of the daily NEP cycle (Richardson et al., 2011; Schaefer et al., 2012; Balzarolo et al., 2014), as expected there is a relatively larger bias for NEP in our simulation. The FORCCHN model underestimates the NEP at most EC sites, this is especially true for mixed and evergreen needleleaf forests since the greatest bias is observed with averaged values being $-0.79 \text{ g C m}^{-2} \text{d}^{-1}$ and $-0.75 \text{ g C m}^{-2} \text{d}^{-1}$, respectively (Fig. 3c, Table 2).

Table 2 reports the number of sites for which the model efficiency (E) is >50%. Balzarolo et al. (2014) note that such a value of E indicates an acceptable level for model's outputs since it means that the simulation explains >50% of the variability of the observations. Overall, the deciduous broadleaf forest sites present a rather large proportion of C flux simulations with E > 50% (100% for GPP, 50% for ER and 62.5% for NEP),

while this happens only once for GPP and never happens for ER and NEP at the evergreen broadleaf forest sites. This further reinforces that FORCCHN model has limitations in reproducing C fluxes in evergreen broadleaf forest.

3.2. Temporal variation at the site level

To investigate the modelling of seasonal variations for different forest types in more detail, we initially compare the 1:1 relationship between observed and simulated GPP, ER and NEP across 37 EC forest sites on monthly time scale (Supplement, Fig. S1–S3), and then four representative sites covering different forest types and different continents (CN-Cha as a mixed forest site in Asia; NL-Loo as an evergreen needleleaf forest site in Europe; US-Ha1 as a deciduous broadleaf forest site in North America and AU-Tum as an evergreen broadleaf forest site

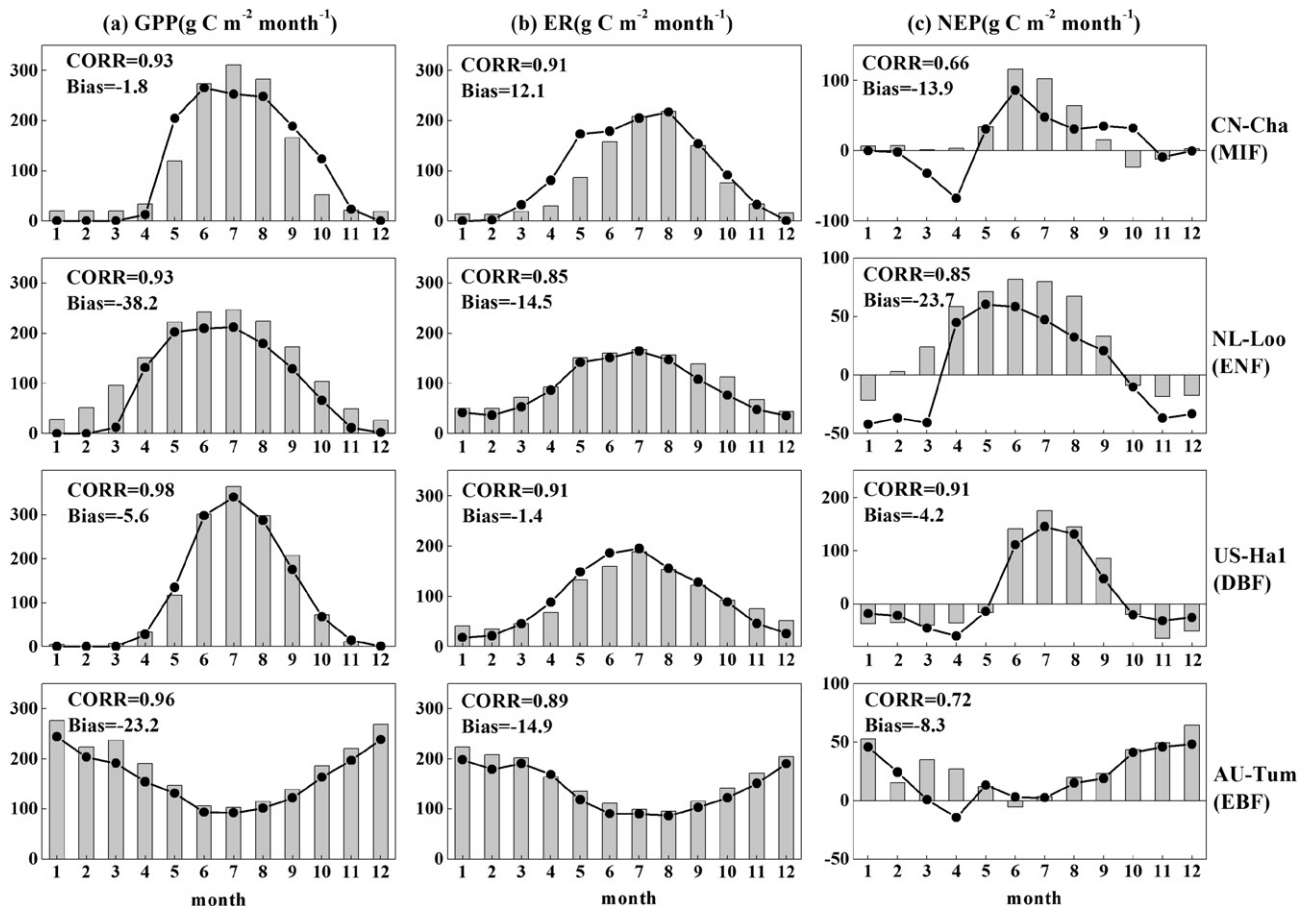


Fig. 4. Monthly variation of observed and simulated (a) GPP, (b) ER and (c) NEP at four EC sites: (from top to bottom) Changbaishan site in China (CN-Cha), Loobos site in Netherlands (NL-Loo), Harvard Forest site in USA (US-Ha1) and Tumbarumba site in Australia (AU-Tum). The grey histogram denotes observation and black dot denotes simulation.

in Oceania) are chosen to analyze seasonal variations of the three C fluxes during the year. Given Fig. 4, the simulations capture the seasonal variation of the observed C fluxes well across four sites with all CORR values being much higher than 0.6, but there is a moderate model bias seen in some months.

For GPP, the magnitudes are markedly underestimated in summer and winter; this is especially true at NL-Loo (evergreen needleleaf forest) and AU-Tum (evergreen broadleaf forest) sites, where the modelled GPP are lower than the observations across all months (Fig. 4a). FORCCHN predicts nearly zero GPP in winter at middle-high latitude EC sites in the Northern Hemisphere (i.e., CN-Cha, NL-Loo and US-Ha1). This result is consistent with previous model studies, such as Suzuki and Ichii (2010), Schaefer et al. (2012).

For ER, simulations also show good skill for the seasonal variation of the flux because of the higher CORR values across four sites. At the Northern Hemisphere site, the simulations and observations perform that the largest flux occurs from June to August and the smallest flux is observed from December to February, and such phenomenon is completely on the contrary at the Southern Hemisphere site (Fig. 4b). In terms of bias, the result derived from ER shows much smaller value when comparing with GPP across four sites.

For NEP, the annual course of positive or negative value is well captured by simulations but FORCCHN markedly underestimates the magnitudes of NEP (Fig. 4c), this is particularly so at NL-Loo (evergreen needleleaf forest) and CN-Cha (mixed forest) sites, where the averaged bias could nearly reach to $-24 \text{ g C m}^{-2} \text{ month}^{-1}$ and $-14 \text{ g C m}^{-2} \text{ month}^{-1}$, respectively.

We further analyze the simulated and observed annual variation of GPP, ER and NEP during the available years across 37 EC forest sites (Supplement, Table S3–S5), and the four representative sites exhibited in Fig. 4 are also selected to examine the model's simulation ability on

annual time scale. Given Fig. 5, the interannual variability of NEP is more difficult to be reproduced than GPP and ER by FORCCHN, this is extremely true at NL-Loo (evergreen needleleaf forest) site, in which case the averaged absolute anomalies of simulated and observed NEP are 105.8% and 32.0%, respectively. Simulated interannual variability of three C fluxes at US-Ha1 (deciduous broadleaf forest) site tend to present great agreement with EC data because the relatively smaller anomaly discrepancies are observed when comparing with other three sites. Due to the limited years being available for comparison, it is hard to analyze the annual variation at CN-Cha (mixed forest) and Au-Tum (evergreen broadleaf forest) sites, although the simulated and observed C fluxes show less anomaly discrepancy as the year processes.

3.3. Simulation performance by Köppen climate classification

According to the Köppen climate classification, there exists six different climate types in our studied EC sites (Supplement, Table S1). Boxplots shown in Fig. 6 report the distribution of the GPP, ER and NEP annual CORR scores for all EC sites grouped by Köppen climate classification. The simulation performances in Dfb, Dfc, Cfa and Cfb climate zones are comparable since FORCCHN always shows the largest CORR scores with a reduced variation for GPP and the smallest correlation values with wide interquartile range for NEP. However, there exists obvious discrepancy between simulations and observations for Csa climate zone with the median CORR values of ER and NEP < 0.5 and with large interquartile ranges. The CORR values are distributed away around the median values and the Csa forest sites show very inconsistent annual CORR values.

Table 3 reports the averaged CORR scores and number of sites with model efficiency (E) higher than 50% for climate classes. On average, FORCCHN shows good skills in simulating C fluxes for forest sites

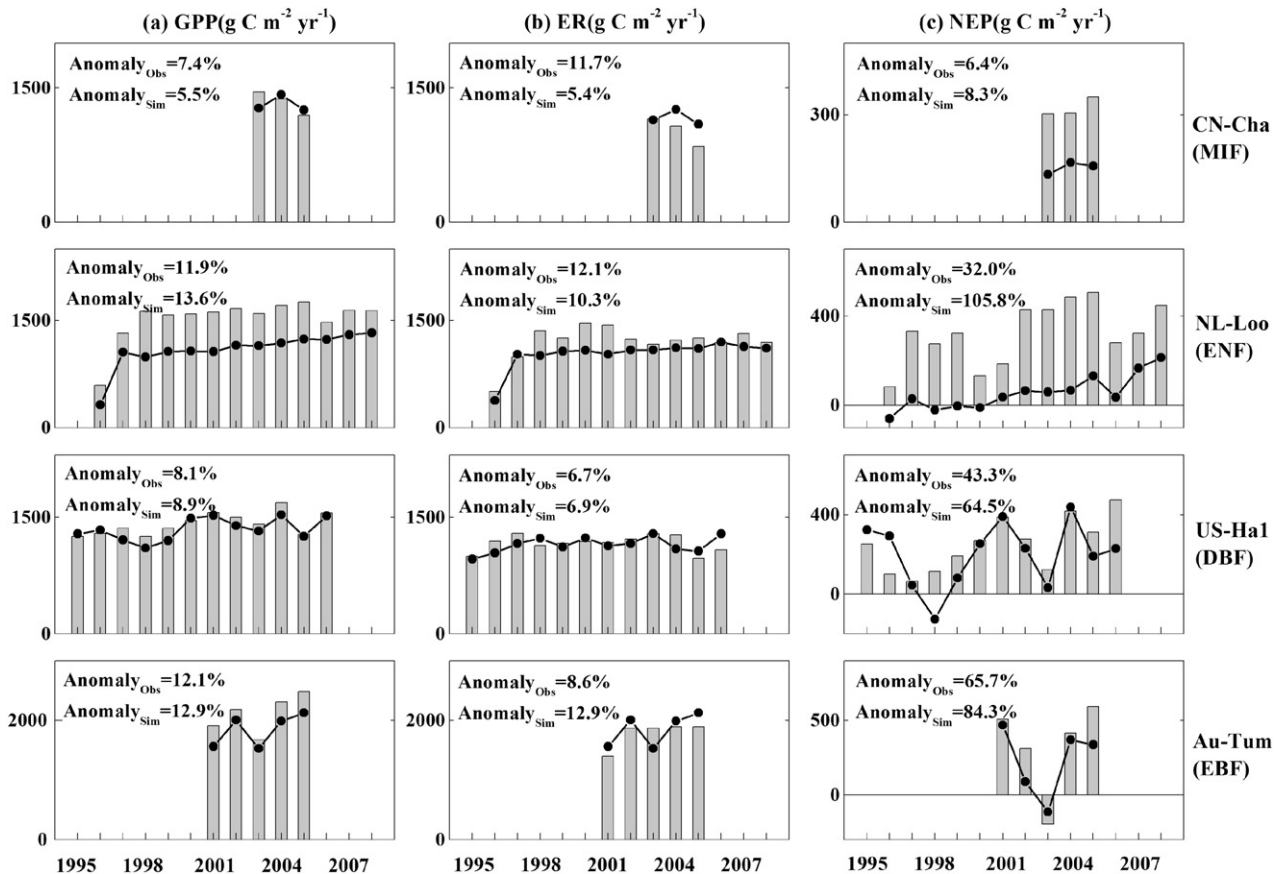


Fig. 5. The same as Fig. 4, but for annual variation. Anomaly_{Obs} and Anomaly_{Sim} are the averaged absolute anomalies of the observed and simulated C fluxes during the available years, respectively. The grey histogram denotes observation and black dot denotes simulation.

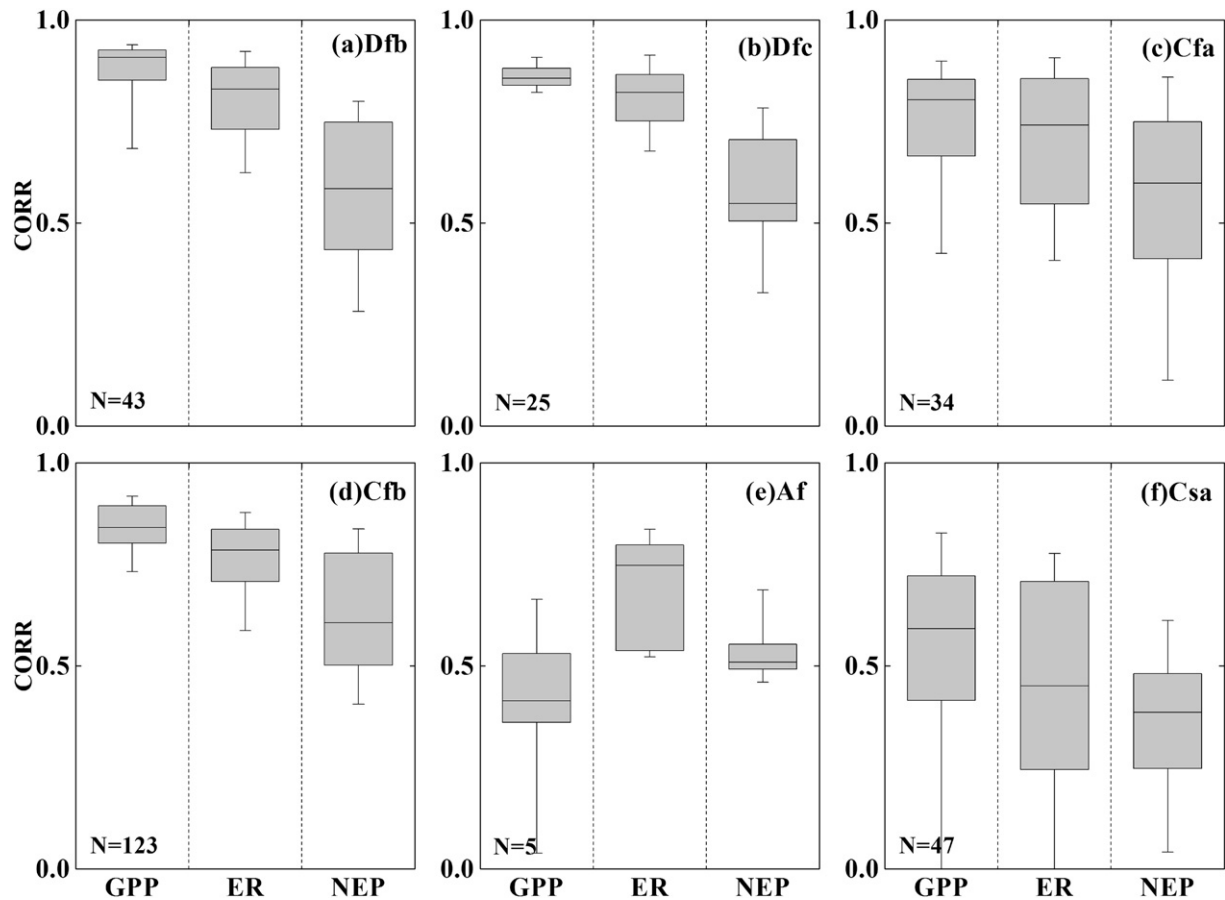


Fig. 6. The same as Fig. 3, but for Köppen climate classification: (a) Dfb-warm summer continental: significant precipitation in all seasons, (b) Dfc-subarctic: severe winter, no dry season, cool summer, (c) Cfa-humid subtropical: mild with no dry season, hot summer, (d) Cfb-marine west coast: mild with no dry season, warm summer, (e) Af-tropical rain forest and (f) Csa-Mediterranean: mild with dry and hot summer. N is number of available years.

located in Dfb, Dfc, Cfa and Cfb climate zones. However, the simulations for Af and Csa Köppen climate classes present poorer CORR scores, and number of sites with E higher than 50% are zero at Af sites and happen only once for ER at Csa sites.

3.4. Global estimation of carbon fluxes

Having tested the model at 37 EC sites to gain an impression of the model's performance (Sections 3.1–3.3), our next objective is to assess the global temporal and spatial patterns of C fluxes in forest ecosystems using FORCCHN model. Here, GLASS-LAI products in 1982 are used to achieve a forest initial condition, such as DBH and canopy height (Supplement, Fig. S4). Moreover, to insure that the allocation proportion of organic carbon in ten soil pools (Table 1) are in equilibrium in FORCCHN, we first spin up the model for 1000 years at each grid and then take the new allocation proportion and soil C storage as model input data to simulate C fluxes for the past 30 years.

Fig. 7 reports the spatial distribution of multi-year averaged GPP, ER and NEP for global forest ecosystems. Overall, GPP and ER are similar with largest fluxes occurring in the equatorial tropics followed by monsoonal subtropical regions (e.g. south and east Asia), and humid temperate regions in eastern North America, western Europe and eastern Oceania. Boreal forests show the smallest fluxes where the main forest type is deciduous needleleaf forest (Fig. 7a, b). The resulting spatial pattern is consistent with the Model Tree Ensemble-based GPP estimations derived from Jung et al. (2011). Note, however, that the GPP derived from FORCCHN for most tropical rain forest is $\sim 300 \text{ g C m}^{-2} \text{ yr}^{-1}$ smaller and for parts of South-Central African $\sim 900 \text{ g C m}^{-2} \text{ yr}^{-1}$ larger than those of Jung et al. (2011), respectively (Ma et al., 2015). In terms of

long-term changes in C fluxes, both GPP and ER present a significant increase ($P < 0.01$) from 1982 to 2011 regardless of forest type (Fig. 8a, b), the forest type with the greatest CO_2 uptake by photosynthesis and CO_2 release by ecosystem respiration are evergreen broadleaf forest, deciduous broadleaf forest and mixed forest, respectively. For global forest ecosystems, the GPP and ER generated by FORCCHN are 1307 ± 140 (mean ± 1 standard deviation) and $1251 \pm 132 \text{ g C m}^{-2} \text{ yr}^{-1}$, and GPP is comparable to the observation-based estimations derived from Beer et al. (2010) for which the averaged GPP of seven estimations is $1305.4 \text{ g C m}^{-2} \text{ yr}^{-1}$. As far as total annual C fluxes are concerned, total GPP and ER of global forest ecosystems are 59.41 ± 5.67 and $57.21 \pm 5.32 \text{ Pg C yr}^{-1}$ (Table 4), respectively, the GPP result is within

Table 3

Performance of the FORCCHN in simulating daily carbon fluxes for Köppen climate classification^a.

Köppen climate	N. site	N. data	GPP		ER		NEP	
			CORR	N. sites E > 50%	CORR	N. sites E > 50%	CORR	N. sites E > 50%
Dfb	5	15,042	0.84	4	0.79	3	0.55	2
Dfc	4	7980	0.72	3	0.79	2	0.61	0
Cfa	6	11,355	0.65	3	0.76	1	0.44	0
Cfb	14	42,683	0.82	10	0.73	6	0.61	4
Af	2	1826	0.45	0	0.73	0	0.57	0
Csa	6	16,271	0.51	0	0.44	1	0.33	0

^a N. site-number of available sites for each Köppen climate classification; N. data-number of available days; CORR-correlation coefficient; N. sites E > 50%-number of sites with model efficiency (E) higher than 50%; Dfb-warm summer continental; Dfc-subarctic: severe winter; Cfa-humid subtropical; Cfb-marine west coast; Af-tropical rain forest; Csa-Mediterranean.

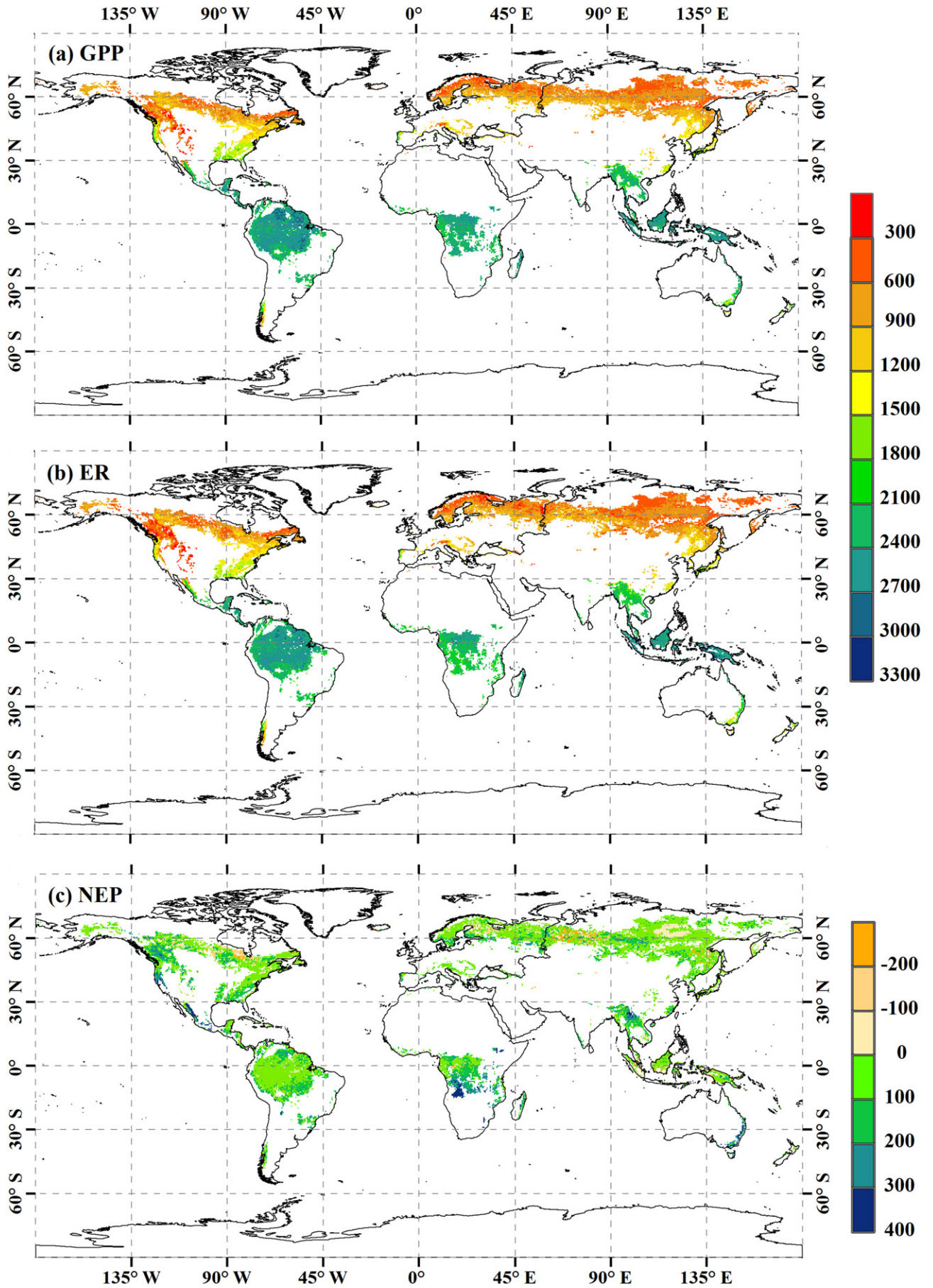


Fig. 7. Simulated by FORCCHN spatial distribution of mean (a) GPP, (b) ER and (c) NEP ($\text{g C m}^{-2} \text{yr}^{-1}$) for global forest ecosystems during 1982–2011.

the range reported by observation-based estimations of 52.61–67.54 Pg C yr⁻¹ (Beer et al., 2010) and satellite-based simulations of 37.59–59.77 Pg C yr⁻¹ (Cai et al., 2014).

NEP, as the difference between GPP and ER, presents more complicated spatial pattern than remaining C fluxes. The largest NEP value occurs 20°–40°S in Africa followed by 15°–30°N in subtropical forest ecosystems. Tropical forest (15°S–15°N) and mid-high latitude (30°–50°N) forests in Northern Hemisphere are also found to be positive values (Fig. 7c). Conversely, there exists a weak negative longitude bands in North of 55°N; presumably in response to the dramatic underestimation of NEP for evergreen needleleaf forest and mixed forest types by FORCCHN (Fig. 3, Table 2). In terms of interannual variation, evergreen broadleaf forest and evergreen needleleaf forest present an obvious NEP increase ($P < 0.01$) from 1982 to 2011, while there exists a significant trend towards reduced NEP as the year progresses for deciduous needleleaf forest (Fig. 8c), indicating that the C sequestration capacity of deciduous needleleaf forest shows decreased tendency from 1982 to 2011. The forest types with the greatest C uptakes are evergreen broadleaf forest, evergreen needleleaf forest and mixed forest, with total NEP values of 1.12 ± 0.52 , 0.54 ± 0.26 and 0.36 ± 0.10 Pg C yr⁻¹, respectively (Table 4). Overall, the global forest ecosystems have been shown to contribute a huge C storage with total NEP being 2.20 ± 0.64 Pg C yr⁻¹, which is close to the C forest sink of 2.4 ± 0.4 Pg C yr⁻¹ globally for 1990–2007 (Pan et al., 2011), and is smaller than the value of 2.33 ± 0.80 Pg C yr⁻¹ computed from residual land sink of the global C budget for 1982–2011 (Le Quéré et al., 2015), and is within the range reported by DGVMs model-based estimations of 0.80–3.34 Pg C yr⁻¹ (Supplement, Fig. S5).

4. Discussion

4.1. Model validation across all EC sites

The model predictions in this study underestimated the GPP based on EC measurements for all forest types (Fig. 3, Table 2), this phenomenon probably arises from several considerations: I. The physiological and ecological characteristics of individual tree are not completely accounted for by PFTs' parameter in FORCCHN (Section 2.2) since the unified parameters could not characterize the growth discrepancies among individual trees. This is the most likely reason why our model predicts a nearly zero GPP at most EC sites from December to March in middle-high latitude. II. Numerous studies have already proved that N deposition mainly has a positive impact on the carbon dioxide uptake by temperate, boreal and subtropical forest ecosystems in the Northern Hemisphere in recent years (Magnani et al., 2007; Pregitzer et al., 2008; Thomas et al., 2010; Yu et al., 2014; Piao et al., 2015), and a recent model evaluation also revealed that not accounting for N deposition resulted in a mean 11% lower net primary productivity (NPP) across European forests by comparing the BIOME-BGC simulations with and without N cycling (Luyssaert et al., 2010). Accordingly, N deposition not taken into account by the FORCCHN model in present study might increase the GPP estimation's uncertainty (Ma et al., 2015); III. Although treated here as “observed GPP”, this is not strictly the observed C flux of the eddy covariance systems but rather estimated from the observed tower-based NEP. The empirical formulation for ecosystem respiration and various gap-filled approaches for net ecosystem exchange can both introduce biases when NEP is processed and partitioned into ER and GPP (Yuan et al., 2014a). Accordingly, the “observed GPP” is likely to affect the uncertainty of model validation.

Besides, we found FORCCHN showed poor performance for the evergreen broadleaf forest, and good performance for deciduous broadleaf forest. This conclusion was supported by recent model evaluations, such as Raczka et al. (2013) and Yuan et al. (2014a). In general, deciduous broadleaf forest demonstrates distinct seasonal dynamics of leaf phenology, and dominating factors of vegetation production can be

explicitly described by model. On the contrary, evergreen broadleaf forest reveals subtle changes in the seasonal leaf phenology, and various environment factors jointly determine plant photosynthesis, which increase the difficulty in modelling.

Although the usage of 37 EC sites in this study are correct in themselves, the global distribution still lacks a full representation of all forest ecosystems for model validation. Particularly most sites are biased to the Northern Hemisphere, with only 4 sites occurring in the Southern Hemisphere and no sites being in African tropical forest (Fig. 1). Hence, further work can be strengthened by including more systematic and objective model evaluation using more EC observation sites.

4.2. Model performance under Mediterranean climate

The difficulties in predicting C fluxes of the Csa forest sites considered in this study (Fig. 6) can be due to the fact that uncertainties in the representation of the water stress characterizing the Csa climate affect the simulations of GPP and ER (Migliavacca et al., 2011; Szczypta et al., 2014). On one hand, drought tolerance parameter in FORCCHN (Supplement, Table S2) is not appropriate enough to represent water stress during summer dry period, and variability in drought tolerance differs substantially among individual species but our model does not consider the discrepancy as we use PFTs for simulation (Section 2.2). On the other hand, as reported by Balzarolo et al. (2014), several environmental factors impact seasonal variability of C fluxes in water limited biomes. In this study, FORCCHN could not totally account for the impacts of environmental factors on C fluxes during summer dry period (Supplement, Fig. S6), which is most likely to generate the poor performance.

In addition, management practices, such as heavy thinning and water harvesting could also increase the modelling difficulties under Mediterranean climate. For example, in Israel, the tree plantations are often supported by building a ‘liman’ (Schiller and Karschon, 1974; Bredemeier, 2011), during the rare but frequently strong precipitation events, the artificial basin of the ‘liman’ fills up by surface flow, and water is forced to infiltrate locally, which indirectly increases actual water input and therefore alleviates the impact of water stress on tree growth. Noted, however, that this process not reflected in our simulation likely causes poor predictions, it is particularly so at IL-Yat site where the peak photosynthetic activity has been observed in early spring (Rotenberg and Yakir, 2010), while FORCCHN predicts the zero GPP throughout the entire cycle of conifer plantation (Supplement, Fig. S1).

4.3. Simulation uncertainty on global scale

The potential uncertainty in estimating C fluxes on global scale may include the following:

- I. Uncertainty from the model. Previous studies (Cramer et al., 1999; Schaefer et al., 2012; Ogotu and Dash, 2013) have shown that different C flux estimates among models are caused by model structural differences (e.g. model assumptions, algorithm simplifications, and parameterizations). For example, a recent study, comparing seven light-use efficiency models against observations from 157 global EC towers, showed substantial disagreement in the estimated GPP among different models (Yuan et al., 2014a). Our findings derive from one carbon budget model (i.e., FORCCHN) driven by one climate forcing dataset. The transfer of our findings to other models might need further examination, since the sensitivity of FORCCHN to the choice of forcing dataset may not be the same as for other models;
- II. Uncertainty from satellite-derived vegetation products. As reported by Beer et al. (2010), the changes in land cover maps caused large discrepancies in global GPP estimates. In the present study, evergreen broadleaf forest exists in south-central Africa

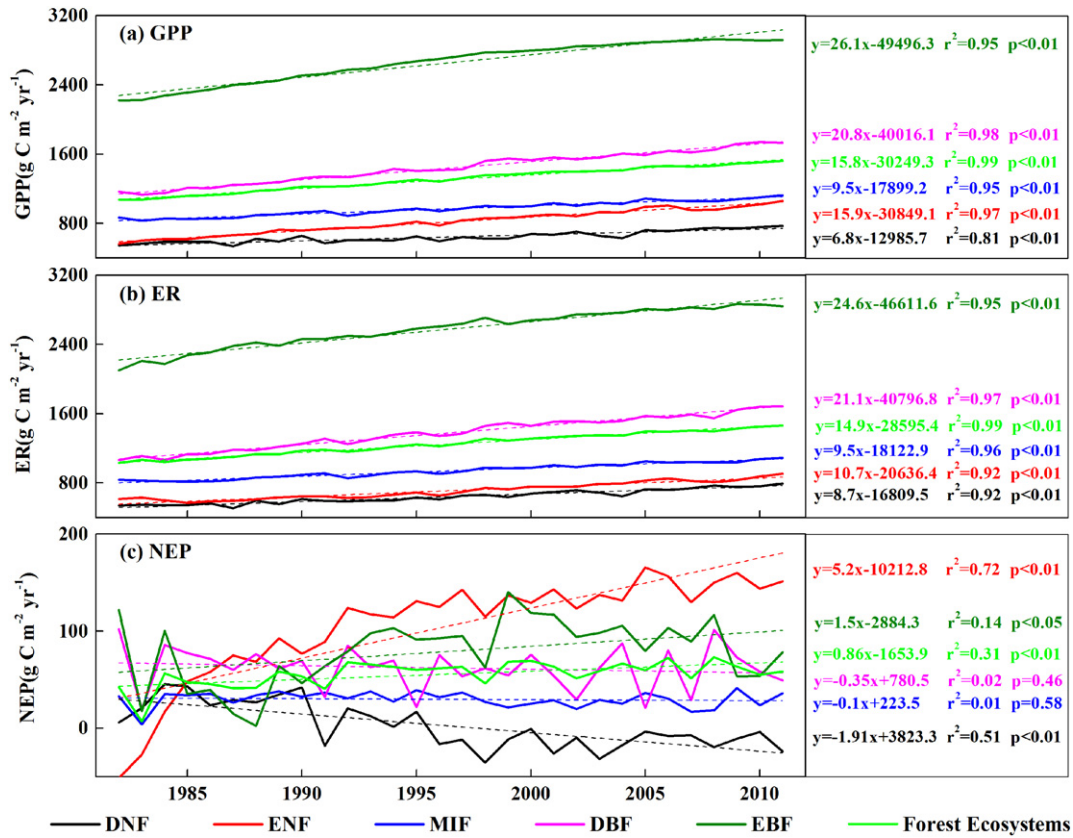


Fig. 8. Simulated by FORCCHN interannual variation of (a) GPP, (b) ER and (c) NEP ($\text{g C m}^{-2} \text{yr}^{-1}$) for different forest types during 1982–2011. The dash line represents the linear regression of the carbon flux in the past 30 years.

based on IGBP-DIS classification scheme (Fig. 1); however, according to GLC2000 and MODIS land cover, the identical land is broadly classified into deciduous broadleaf forest and savanna, respectively. Obviously, the inconsistent forest areas would directly increase the estimation uncertainty of total C fluxes. Furthermore, FORCCHN depends on satellite-derived vegetation products such as LAI, which have been reported to increase errors in C flux estimation (Ryu et al., 2011; Yuan et al., 2014b). In our model, the satellite-derived LAI data is used to initialize the tree numbers and individual tree's growth status in the starting year of simulation, the discrepancies among different LAI products might generate different initialized results, which would potentially affect the estimation of total C flux in forest ecosystems on plot scale.

III. Uncertainty from climate input. Uncertainties in C model estimates are often considered to be largely induced by biases in forcing climate data (Zhao et al., 2006; Barman et al., 2014). A comparison between in-situ and gridded forcing variables confirmed that Princeton University data set present a great

agreement with the EC tower-based observations because of the relatively dense measurement network, however, the errors are likely to be larger in some other parts of the world where measurement networks are less developed (Yebra et al., 2015). Therefore, to reduce the uncertainty, further efforts should be focused on the estimation of global C fluxes using an ensemble of climate input (e.g. MERRY, ERA-Interim, and NCEP/NCAR).

4.4. Other limitations

Land Use and Land Cover Change (LULCC) is a required factor to quantify the global C cycle, the net flux of carbon from LULCC is $1.10 \pm 0.11 \text{ Pg C yr}^{-1}$ from 2000 to 2009 (Houghton et al., 2012), accounting for 12.5% of anthropogenic carbon emissions (Friedlingstein et al., 2010). LULCC not included in the study is most likely cause of the C estimation's uncertainty on the global scale. In addition, pests and diseases are additional weaknesses of the model because these factors might counteract the effects of the anticipated mean warming and

Table 4
Simulated by FORCCHN mean annual (1982– 2011) carbon fluxes for different forest types on global scale.^a

	ENF	EBF	DNF	DBF	MIF	Forest ecosystems
Mean ($\text{g C m}^{-2} \text{yr}^{-1}$)						
GPP	818 ± 141	2657 ± 233	645 ± 65	1442 ± 183	971 ± 85	1307 ± 140
ER	712 ± 98	2578 ± 222	643 ± 80	1380 ± 188	941 ± 86	1251 ± 132
NEP	106 ± 53	79 ± 34	2 ± 23	62 ± 23	30 ± 8	56 ± 13
Total (Pg C yr^{-1})						
GPP	4.29 ± 0.73	39.98 ± 3.52	1.33 ± 0.13	2.87 ± 0.37	10.95 ± 0.97	59.41 ± 5.67
ER	3.75 ± 0.52	38.81 ± 3.32	1.32 ± 0.17	2.75 ± 0.38	10.59 ± 1.00	57.21 ± 5.32
NEP	0.54 ± 0.26	1.12 ± 0.52	0.01 ± 0.05	0.12 ± 0.04	0.36 ± 0.10	2.20 ± 0.64

^a Uncertainty estimates refer to one standard deviation and are derived from the spread of 1982– 2011. Forest ecosystems represent all five categories.

lengthening of the growing season and reduce the productivity of the ecosystems, reversing sinks to sources (Zhao et al., 2012). Moreover, the processes of canopy interception, surface runoff and actual evapotranspiration, which could impact the simulated accuracy of the forest biomass, should also be coupled to FORCCHN in future studies.

5. Conclusion

Based on an individual tree-based model FORCCHN, we initially examined the model performance using CO₂ flux measurements from 37 EC sites, and then estimated the C fluxes of forest ecosystems on global scale over the 1982–2011 period. FORCCHN underestimated GPP and slightly overestimated ER, and GPP is the major reason for the underestimation of NEP in forest ecosystems across most EC sites. On average, model showed good performance for deciduous broadleaf forest sites and poor performance for evergreen broadleaf forest sites. All simulations showed some limitations in capturing GPP, ER and NEP seasonality for Mediterranean climate. Application of FORCCHN gave an annual total GPP and ER of 59.41 ± 5.67 and 57.21 ± 5.32 Pg C yr⁻¹ from 1982 to 2011, and global forest ecosystems have been shown to contribute a huge C storage for the same period, with total NEP being 2.20 ± 0.64 Pg C yr⁻¹, which is also comparable to the results reported by related studies. Note, however, that the global distribution of EC sites in the study still lacks a full representation of all forest ecosystems for model validation, and following study should be strengthened by including more model evaluation using more EC observation sites to further convince in the rationality of using FORCCHN on the global scale.

Acknowledgments

This study was financially supported by the National Natural Science Foundation of China (grant numbers: 41330527, 31570473) and Fundamental Research Funds for the Central Universities (grant number: 2662016QD041). Prof. Herman H. Shugart was supported by a grant from the Center for Global Inquiry and Innovation at the University of Virginia. Special thanks to Prof. Dan Yakir and Prof. Michael Sprintsin for useful discussions and suggestions on the Yatir forest in Israel.

Appendix A. Supplementary data

Supplementary data to this article can be found online at <http://dx.doi.org/10.1016/j.scitotenv.2017.02.073>.

References

Balzarolo, M., Boussetta, S., Balsamo, G., Beljaars, A., Maignan, F., Calvet, J.C., Lafont, S., Barbu, A., Poulter, B., Chevallier, F., Szczypka, C., Papale, D., 2014. Evaluating the potential of large-scale simulations to predict carbon fluxes of terrestrial ecosystems over a European Eddy covariance network. *Biogeosciences* 11, 2661–2678.

Barman, R., Jain, A.K., Liang, M., 2014. Climate-driven uncertainties in modeling terrestrial gross primary production: a site level to global-scale analysis. *Glob. Chang. Biol.* 20, 1394–1411.

Beer, C., Reichstein, M., Tomelleri, E., Ciais, P., Jung, M., Carvalhais, N., Rodenbeck, C., Arain, M.A., Baldocchi, D., Bonan, G.B., Bondeau, A., Cescatti, A., Lasslop, G., Lindroth, A., Lomas, M., Luysaert, S., Margolis, H., Oleson, K.W., Rouspard, O., Veenendaal, E., Viovy, N., Williams, C., Woodward, F.I., Papale, D., 2010. Terrestrial gross carbon dioxide uptake: global distribution and covariation with climate. *Science* 329, 834–838.

Bredemeier, M., 2011. Forest, climate and water issues in Europe. *Ecohydrology* 4, 159–167.

Cai, W., Yuan, W., Liang, S., Liu, S., Dong, W., Chen, Y., Liu, D., Zhang, H., 2014. Large differences in terrestrial vegetation production derived from satellite-based light use efficiency models. *Remote Sens.* 6, 8945–8965.

Cramer, W., Kicklighter, D.W., Bondeau, A., Moore, B., Churkina, C., Nemry, B., Ruimy, A., Schiess, A.L., 1999. Comparing global models of terrestrial net primary productivity NPP: overview and key results. *Glob. Chang. Biol.* 5, 1–15.

Foley, J.A., 1994. Net primary productivity in the terrestrial biosphere: the application of a global model. *J. Geophys. Res.* 99 (D10), 20773–20783.

Friedlingstein, P., Houghton, R., Marland, G., Hackler, J., Boden, T.A., Conway, T.J., Canadell, J.G., Raupach, M.R., Ciais, P., Le Quééré, C., 2010. Update on CO₂ emissions. *Nat. Geosci.* 3, 811–812.

Friend, A.D., Stevens, A.K., Knox, R.G., Cannel, M.G.R., 1997. A process-based, terrestrial biosphere model of ecosystem dynamics (hybrid v3.0). *Ecol. Model.* 95, 249–287.

Global Soil Data Task Group. (2000). Global Gridded Surfaces of Selected Soil Characteristics (IGBP-DIS) Dataset. Available on-line [<http://daac.ornl.gov/>] from Oak Ridge National Laboratory Distributed Active Archive Center, Oak Ridge, Tennessee, U.S.A.

Gray, A.N., Whittier, T.R., 2014. Carbon stocks and changes on Pacific northwest national forests and the role of disturbance, management, and growth. *For. Ecol. Manag.* 328, 167–178.

Houghton, R.A., House, J.I., Pongratz, J., van der Werf, G.R., DeFries, R.S., Hansen, M.C., Le Quééré, C., Ramankutty, N., 2012. Carbon emissions from land use and land-cover change. *Biogeosciences* 9, 5125–5142.

Jung, M., Reichstein, M., Margolis, H.A., Cescatti, A., Richardson, A.D., Arain, M.A., Arneth, A., Bernhofer, C., Bonal, D., Chen, J., Gianelle, D., Gobron, N., Kiely, G., Kutsch, W., Lasslop, G., Law, B.E., Lindroth, A., Merbold, L., Montagnani, L., Moors, E.J., Papale, D., Sottocornola, M., Vaccari, F., Williams, C., 2011. Global patterns of land-atmosphere fluxes of carbon dioxide, latent heat, and sensible heat derived from eddy covariance, satellite, and meteorological observations. *J. Geophys. Res.* 116, G00J07.

King, A.W., Post, W.M., Wullschlegel, S.D., 1997. The potential response of terrestrial carbon storage to changes of climate and atmospheric CO₂. *Clim. Chang.* 35, 199–227.

Kirschbaum, M.U.F., Paul, K.I., 2002. Modelling C and N dynamics in forest soils with a modified version of the CENTURY model. *Soil Biol. Biochem.* 34, 341–354.

Krinner, G., Viovy, N., de Noblet-Ducoudré, N., Ogée, J., Polcher, J., Friedlingstein, P., Ciais, P., Sitch, S., Prentice, I.C., 2005. A dynamic global vegetation model for studies of the coupled atmosphere-biosphere system. *Glob. Biogeochem. Cycles* 19, GB1015.

Le Quééré, C., Raupach, M.R., Canadell, J.G., Marland, G., Bopp, L., Ciais, P., Conway, T.J., Doney, S.C., Feely, R.A., Foster, P., Friedlingstein, P., Gurney, K., Houghton, R.A., House, J.I., Huntingford, C., Levy, P.E., Lomas, M.R., Majkut, J., Metz, N., Ometto, J.P., Peters, G.P., Prentice, I.C., Randerson, J.T., Running, S.W., Sarmiento, J.L., Schuster, U., Sitch, S., Takahashi, T., Viovy, N., van der Werf, G.R., Woodward, F.I., 2009. Trends in the sources and sinks of carbon dioxide. *Nat. Geosci.* 2, 831–836.

Le Quééré, C., Moriarty, R., Andrew, R.M., Peters, G.P., Ciais, P., Friedlingstein, P., Jones, S.D., Sitch, S., Tans, P., Arneth, A., Boden, T.A., Bopp, L., Bozec, Y., Canadell, J.G., Chevallier, F., Cosca, C.E., Harris, I., Hoppema, M., Houghton, R.A., House, J.I., Jain, A.K., Johannessen, T., Kato, E., Keeling, R.F., Kitidis, V., Klein Goldewijk, K., Koven, C., Landa, C., Landschützer, P., Lenton, A., Lima, I.D., Marland, G.H., Mathis, J.T., Metz, N., Nojiri, Y., Olsen, A., Ono, T., Peters, W., Pfeil, B., Poulter, B., Raupach, M.R., Regnier, P., Rodenbeck, C., Saito, S., Salsbury, J.E., Schuster, U., Schwinger, J., Séférian, R., Segsneider, J., Steinhoff, T., Stocker, B.D., Sutton, A.J., Takahashi, T., Tilbrook, B., van der Werf, G.R., Viovy, N., Wang, Y.P., Wanninkhof, R., Wiltshire, A., Zeng, N., 2015. Global carbon budget 2014. *Earth Syst. Sci. Data* 7, 47–85.

Liang, S., Zhao, X., Liu, S., Yuan, W., Cheng, X., Xiao, Z., Zhang, X., Liu, Q., Cheng, J., Tang, H., Qu, Y., Bo, Y., Qu, Y., Ren, H., Townshend, J., 2013. A long-term global land surface satellite (GLASS) data-set for environmental studies. *Int. J. Digital Earth* 6, 5–33.

Loveland, T., J. Brown, D. Ohlen, B. Reed, Z. Zhu, L. Yang and S. Howard. (2009). ISLSCP II IGBP DISCover and SiB Land Cover, 1992–1993. Available on-line [<http://daac.ornl.gov/>] from Oak Ridge National Laboratory Distributed Active Archive Center, Oak Ridge, Tennessee, U.S.A.

Luysaert, S., Ciais, P., Piao, S.L., Schulze, E.D., Jung, M., Zaehle, S., Schelhaas, M.J., Reichstein, M., Churkina, G., Papale, D., Abril, G., Beer, C., Grace, J., Loustau, D., Matteucci, G., Magnani, F., Nabuurs, G.J., Verbeek, H., Sulkava, M., van der Werf, G.R., Janssens, I.A., 2010. The European carbon balance. Part 3: forests. *Glob. Chang. Biol.* 16, 1429–1450.

Ma, J., Yan, X., Dong, W., Chou, J., 2015. Gross primary production of global forest ecosystems has been overestimated. *Sci. Report.* 5, 10820.

Magnani, F., Mencuccini, M., Borghetti, M., Bernigier, P., Berninger, F., Delzon, S., Grelle, A., Hari, P., Jarvis, P.G., Kolar, P., Kowalski, A.S., Lankreijer, H., Law, B.E., Lindroth, A., Loustau, D., Manca, G., Moncrieff, J.B., Rayment, M., Tedeschi, V., Valentini, R., Grace, J., 2007. The human footprint in the carbon cycle of temperate and boreal forests. *Nature* 447, 848–850.

McGuire, A.D., Melillo, J.M., Joyce, L.A., Kicklighter, D.W., Grace, A.L., Moore, B., Vorosmarty, C.J., 1992. Interactions between carbon and nitrogen dynamics in estimating net primary productivity for potential vegetation in North America. *Glob. Biogeochem. Cycles* 6, 101–124.

McKinley, D.C., Ryan, M.G., Birdsey, R.A., Giardina, C.P., Harmon, M.E., Heath, L.S., Houghton, R.A., Jackson, R.B., Morrison, J.F., Murray, B.C., Pataki, D.E., Skog, K.E., 2011. A synthesis of current knowledge on forests and carbon storage in the United States. *Ecol. Appl.* 21, 1902–1924.

Migliavacca, M., Reichstein, M., Richardson, A.D., Colombo, R., Sutton, M.A., Lasslop, G., Tomelleri, E., Wohlfahrt, G., Carvalhais, N., Cescatti, A., Mahecha, M.D., Montagnani, L., Papale, D., Zaehle, S., Arain, A., Arneth, A., Black, T.A., Carrara, A., Dore, S., Gianelle, D., Helfter, C., Hollinger, D., Kutsch, W.L., Lafleur, P.M., Nouvellon, Y., Rebmann, C., Da Rocha, H.R., Rodeghiero, M., Rouspard, O., Sebastião, M.-T., Seufert, G., Soussana, J.-F., Van Der Molen, M.K., 2011. Semi empirical modeling of abiotic and biotic factors controlling ecosystem respiration across eddy covariance sites. *Glob. Chang. Biol.* 17, 390–409.

Nachtergaele, F., Van Velthuyzen, H., Verelst, L., Wiberg, D., 2012. Manual Harmonized World Soil Database v1.2 February 2012.

Ogutu, B.O., Dash, J., 2013. Assessing the capacity of three production efficiency models in simulating gross carbon uptake across multiple biomes in conterminous USA. *Agric. For. Meteorol.* 174–175, 158–169.

Pan, Y., Birdsey, R.A., Fang, J., Houghton, R., Kauppi, P.E., Kurz, W.A., Phillips, O.L., Shvidenko, A., Lewis, S.L., Canadell, J.G., Ciais, P., Jackson, R.B., Pacala, S.W., McGuire, A.D., Piao, S., Rautiainen, A., Sitch, S., Hayes, D., 2011. A large and persistent carbon sink in the world's forests. *Science* 333, 988–993.

Papale, D., Valentini, R., 2003. A new assessment of European forests carbon exchanges by eddy fluxes and artificial neural network spatialization. *Glob. Chang. Biol.* 9, 525–535.

Papale, D., Reichstein, M., Aubinet, M., Canfora, E., Bernhofer, C., Kutsch, W., Longdoz, B., Rambal, S., Valentini, R., Vesala, T., Yakir, D., 2006. Towards a standardized processing of net ecosystem exchange measured with eddy covariance technique: algorithms and uncertainty estimation. *Biogeosciences* 3, 571–583.

Parton, W.J., Scurlock, J.M.O., Ojima, D.S., Gilmanov, T.G., Scholes, R.J., Schimel, D.S., Kirchner, T., Menaut, J.C., Seastedt, T., Moya, E.G., Kamalrut, A., Kinyamaro, J.I.,

1993. Observations and modeling of biomass and soil organic matter dynamics for the grassland biome worldwide. *Glob. Biogeochem. Cycles* 7, 785–809.
- Peng, C., Liu, J., Dang, Q., Apps, M.J., Jiang, H., 2002. TRIPLEX: a generic hybrid model for predicting forest growth and carbon and nitrogen dynamics. *Ecol. Model.* 153, 109–130.
- Piao, S., Yin, G., Tan, J., Cheng, L., Huang, M., Li, Y., Liu, R., Mao, J., Myneni, R.B., Peng, S., Poulter, B., Shi, X., Xiao, Z., Zeng, N., Zeng, Z., Wang, Y., 2015. Detection and attribution of vegetation greening trend in China over the last 30 years. *Glob. Chang. Biol.* 21, 1601–1609.
- Potter, C.S., Randerson, J.T., Field, C.B., Matson, P.A., Vitousek, P.M., Mooney, H.A., Klooster, S.A., 1993. Terrestrial ecosystem production: a process model based on global satellite and surface data. *Glob. Biogeochem. Cycles* 7, 811–841.
- Pregitzer, K.S., Burton, A.J., Zak, D.R., Talhelm, A.F., 2008. Simulated chronic nitrogen deposition increases carbon storage in northern temperate forests. *Glob. Chang. Biol.* 14, 142–153.
- Raczka, B.M., Davis, K.J., Huntzinger, D.N., Neilson, R., Poulter, B., Richardson, A., Xiao, J.F., Baker, I., Ciais, P., Keenan, T.F., Law, B., Post, W.M., Ricciuto, D., Schaefer, K., Tian, H.Q., Tomelleri, E., Verbeeck, H., Viovy, N., 2013. Evaluation of continental carbon cycle simulations with north American flux tower observations. *Ecol. Monogr.* 83, 531–556.
- Reichstein, M., Falge, E., Baldocchi, D., Papale, D., Aubinet, M., Berbigier, P., Bernhofer, C., Buchmann, N., Gilmanov, T., Granier, A., Grunwald, T., Havrankova, K., Ilvesniemi, H., Janous, D., Knohl, A., Laurila, T., Lohila, A., Loustau, D., Matteucci, G., Meyers, T., Miglietta, F., Ourcival, J.-M., Pumpanen, J., Rambal, S., Rotenberg, E., Sanz, M., Tenhunen, J., Seufert, G., Vaccari, F., Vesala, T., Yakir, D., Valentini, R., 2005. On the separation of net ecosystem exchange into assimilation and ecosystem respiration: review and improved algorithm. *Glob. Chang. Biol.* 11, 1424–1439.
- Richardson, A.D., Dail, D.B., Hollinger, D.Y., 2011. Leaf area index uncertainty estimates for model–data fusion applications. *Agric. For. Meteorol.* 151, 1287–1292.
- Rotenberg, E., Yakir, D., 2010. Contribution of semi-arid forests to the climate system. *Science* 327, 451–454.
- Running, S., Hunt, E., 1993. Generalization of a forest ecosystem process model for other biomes, BIOME-BGC, and an application for global scale models. *Scaling Physiological Processes: Leaf to Globe*. Academic Press, San Diego, CA, USA, pp. 141–158.
- Russell, M., Domke, G.M., Woodall, C.W., D'Amato, A.W., 2015. Comparisons of allometric and climate-derived estimates of tree coarse root carbon stocks in forest of the United States. *Carbon Balance Manage.* 10 (1), 20.
- Ryu, Y., Baldocchi, D.D., Kobayashi, H., van Ingen, C., Li, J., Black, T.A., Beringer, J., van Gorsel, E., Knohl, A., Law, B.E., Rouspard, O., 2011. Integration of MODIS land and atmosphere products with a coupled-process model to estimate gross primary productivity and evapotranspiration from 1 km to global scales. *Glob. Biogeochem. Cycles* 25, GB4017.
- Schaefer, K., Schwalm, C.R., Williams, C., Arain, M.A., Barr, A., Chen, J.M., Davis, K.J., Dimitrov, D., Hilton, T.W., Hollinger, D.Y., Humphreys, E., Poulter, B., Raczka, B.M., Richardson, A.D., Sahoo, A., Thornton, P., Vargas, R., Verbeeck, H., Anderson, R., Baker, I., Black, T.A., Bolstad, P., Chen, J., Curtis, P.S., Desai, A.R., Dietze, M., Dragoni, D., Gough, C., Grant, R.F., Gu, L., Jain, A., Kucharik, C., Law, B., Liu, S., Lokipitiya, E., Margolis, H.A., Matamala, R., McCaughey, J.H., Monson, R., Munger, J.W., Oechel, W., Peng, C., Price, D.T., Ricciuto, D., Riley, W.J., Roulet, N., Tian, H., Tonitto, C., Torn, M., Weng, E., Zhou, X., 2012. A model–data comparison of gross primary productivity: results from the North American carbon program site synthesis. *J. Geophys. Res.* 117, G03010.
- Schiller, G., Karschon, R., 1974. Microclimate and recreational value of tree plantings in deserts. *Landscape Planning* 1, 329–337.
- Seidl, R., Spies, T.A., Rammer, W., Steel, E.A., Pabst, R.J., Olsen, K., 2012. Multi-scale drivers of spatial variation in old-growth forest carbon density disentangled with lidar and an individual-based landscape model. *Ecosystems* 15, 1321–1335.
- Sellers, P.J., Randall, D.A., Collatz, G.J., Berry, J.A., Field, C.B., Dazlich, D.A., Zhang, C., Collelo, G.D., Bounoua, L., 1996. A revised land surface parameterization (SiB2) for atmospheric GCMs. Part I: model formulation. *J. Clim.* 9, 676–705.
- Sheffield, J., Gotetiand, G., Wood, E.F., 2006. Development of a 50-year high-resolution global dataset of meteorological forcings for land surface modeling. *J. Clim.* 19, 3088–3111.
- Shugart, H.H., Asner, G.P., Fischer, R., Huth, A., Knapp, N., Le Toan, T., Shuman, J.K., 2015. Computer and remote-sensing infrastructure to enhance large-scale testing of individual-based forest models. *Front. Ecol. Environ.* 13, 503–511.
- Sitch, S., Smith, B., Prentice, I.C., Arneeth, A., Bondeau, A., Cramer, W., Kaplan, J.O., Levis, S., Lucht, W., Sykes, M.T., Thonicke, K., Venevsky, S., 2003. Evaluation of ecosystem dynamics, plant geography and terrestrial carbon cycling in the LPJ dynamic global vegetation model. *Glob. Chang. Biol.* 9, 161–185.
- Smith, B., Prentice, I.C., Sykes, M.T., 2001. Representation of vegetation dynamics in the modelling of terrestrial ecosystems: comparing two contrasting approaches within European climate space. *Glob. Ecol. Biogeogr.* 10, 621–638.
- Song, C., Woodcock, C.E., 2003. A regional forest ecosystem carbon budget model: impacts of forest age structure and land use history. *Ecol. Model.* 164, 33–47.
- Suzuki, T., Ichii, K., 2010. Evaluation of a terrestrial carbon cycle sub model in an Earth system model using networks of eddy covariance observations. *Tellus B* 62, 729–742.
- Szczypta, C., Calvet, J.C., Maignan, F., Dorigo, W., Baretand, F., Ciais, P., 2014. Suitability of modelled and remotely sensed essential climate variables for monitoring Euro-Mediterranean droughts. *Geosci. Model Dev.* 7, 931–946.
- Thomas, R.Q., Canham, C.D., Weathers, K.C., Goodale, C.L., 2010. Increased tree carbon storage in response to nitrogen deposition in the US. *Nat. Geosci.* 3, 229–244.
- Weglarczyk, S., 1998. The interdependence and applicability of some statistical quality measures for hydrological models. *J. Hydrol.* 206, 98–103.
- White, M.K., Gower, S.T., Ahl, D.E., 2005. Life cycle inventories of round wood production in northern Wisconsin: inputs into an industrial forest carbon budget. *For. Ecol. Manag.* 219, 13–28.
- Yan, X., Zhao, J., 2007. Establishing and validating individual-based carbon budget model FORCCHN of forest ecosystems in China. *Acta Ecol. Sin.* 27, 2684–2694.
- Yebara, M., Van Dijk, A., Leuning, R., Guerschman, J., 2015. Global vegetation gross primary production estimation using satellite-derived light use efficiency and canopy conductance. *Remote Sens. Environ.* 163, 206–216.
- Yu, G., Chen, Z., Piao, S., Peng, C., Ciais, P., Wang, Q., Li, X., Zhu, X., 2014. High carbon dioxide uptake by subtropical forest ecosystems in the East Asia monsoon region. *Proc. Natl. Acad. Sci. U. S. A.* 111, 4910–4915.
- Yuan, W., Cai, W., Xia, J., Chen, J., Liu, S., Dong, W., Merbold, L., Law, B., Arain, A., Beringer, J., Bernhofer, C., Black, A., Blanken, P.D., Cescatti, A., Chen, Y., Francois, L., Gianelle, D., Janssen, I.A., Jung, M., Kato, T., Kiely, G., Liu, D., Marcolla, B., Montagnani, L., Raschi, A., Rouspard, O., Varlagin, A., Wohlfahrt, G., 2014a. Global comparison of light use efficiency models for simulating terrestrial vegetation gross primary production based on the LaThuile database. *Agric. For. Meteorol.* 192–193, 108–120.
- Yuan, W., Liu, S., Dong, W., Liang, S., Zhao, S., Chen, J., Xu, W., Li, X., Barr, A., Black, T.A., Yan, W., Goulden, M.L., Kulmala, L., Lindroth, A., Margolis, H.A., Matsuura, Y., Moors, E., van der Molen, M., Ohta, T., Pilegaard, K., Varlagin, A., Vesala, T., 2014b. Differentiating moss from higher plants is critical in studying the carbon cycle of the boreal biome. *Nat. Commun.* 5, 4270.
- Zhao, M., Running, S.W., Nemani, R.R., 2006. Sensitivity of moderate resolution imaging Spectroradiometer (MODIS) terrestrial primary production to the accuracy of meteorological reanalyses. *J. Geophys. Res.* 111, G01002.
- Zhao, J., Yan, X., Guo, J., Jia, G., 2012. Evaluating spatial-temporal dynamics of net primary productivity of different forest types in northeastern China based on improved FORCCHN. *PLoS One* 7, e4813.